

Microstructural Characterization of Burnable Absorber Materials Being Evaluated for Application in LEU U-Mo Fuel Plates

RRFM 2011

D. Keiser, Jr.
J. Jue
I. Glagolenko
G. Moore
C. Clark
B. Rabin
A. Ewh
B. Yao
Y. H. Sohn
T. Totev
T. Wiencek

March 2011

This is a preprint of a paper intended for publication in a journal or proceedings. Since changes may be made before publication, this preprint should not be cited or reproduced without permission of the author. This document was prepared as an account of work sponsored by an agency of the United States Government. Neither the United States Government nor any agency thereof, or any of their employees, makes any warranty, expressed or implied, or assumes any legal liability or responsibility for any third party's use, or the results of such use, of any information, apparatus, product or process disclosed in this report, or represents that its use by such third party would not infringe privately owned rights. The views expressed in this paper are not necessarily those of the United States Government or the sponsoring agency.

The INL is a
U.S. Department of Energy
National Laboratory
operated by
Battelle Energy Alliance



MICROSTRUCTURAL CHARACTERIZATION OF BURNABLE ABSORBER MATERIALS BEING EVALUATED FOR APPLICATION IN LEU U-MO FUEL PLATES

D. KEISER, JR.¹, J. JUE¹, I. GLAGOLENKO¹, G. MOORE¹, C. CLARK¹, B. RABIN¹,
A. EWH², B. YAO², Y. H. SOHN², T. TOTEV³, AND T. WIENCEK³

¹ *Nuclear Fuels and Materials Division, Idaho National Laboratory
P. O. Box 1625, Idaho Falls, Idaho 83403 USA*

² *University of Central Florida
P. O. Box 162450, Orlando, FL 32816 USA*

³ *Argonne National Laboratory, Argonne, Illinois 60439 – USA*

ABSTRACT

The starting microstructure of a fuel plate will impact how it performs during irradiation. This includes any burnable absorber materials that may be added to a dispersion or monolithic fuel plate to compensate for excess reactivity and/or to flatten the radial power profile. The borated compounds B₄C, ZrB₂, and Al-B alloys have been selected for testing in the ATR as part of the RERTR-13 test, and to support completion of this test, microstructural characterization has been performed on the samples in the as-fabricated condition. This paper will discuss the results of optical metallography, scanning electron microscopy, and transmission electron microscopy analyses that have been performed. Overall, there was a fairly significant difference in how the boron-containing phases were distributed in the various samples. The ZrB₂ and B₄C samples had the most uniform distribution of the boron-containing phases. The HIP process used to fabricate the final plate samples effectively closes porosity that was present in some of the foil samples in the as-rolled condition.

1. Introduction

Burnable absorbers (BA) are used in a reactor fuel plate when it is necessary to suppress excess initial reactivity in a fuel and/or to flatten the radial power profile within a fuel element. In ATR and HFIR fuel elements, B₄C is currently used as the burnable absorber [1,2]. As part of the development of low-enriched U-Mo fuel, it is of interest to identify BA material(s) that can be employed for the reactors where the use of such a material is required and also to identify the best methodology of incorporating the material into the fuel plate (particularly for the monolithic fuel) such that there will be no impact of the BA material on the mechanical integrity of the fuel plate during irradiation.

The RERTR-13 reactor experiment being performed in the Advance Test Reactor (ATR) (see Table 1) will test BA-containing samples where the phases that contain boron (B), are B₄C, ZrB₂, or AlB₂. The test is comprised of 28 plates (8 non-fueled material test plates, 8 dispersion plates, and 12 monolithic plates). The B-10 concentrations employed in the materials are prototypic of what would be employed in LEU ATR plates [1]. The prime phenomena of interest in these plates are helium behavior, fuel swelling, blister anneal failure temperature and interaction layer behavior. In order to understand the effects of irradiation, it is necessary to perform detailed pre-test characterization on as-fabricated samples. The pre-test characterization was comprised of optical metallography (OM), scanning electron microscopy (SEM), and transmission electron microscopy (TEM) analyses. This paper will describe the

microstructures that were observed and will focus on the morphology and distribution of the phases that contain the boron.

Table 1. RERTR-13 Experiment Matrix.

ID	Capsule	Column 1	Column 2	Column 3	Column 4
13-A	Top	A-1	A-2	A-3	A-4
		U-7Mo + B ₄ C dispersion in Al-4 wt% Si, U235-25%	U-7Mo + B ₄ C dispersion in Al-4 wt% Si, U235-69%	U-7Mo + ZrB ₂ dispersion in Al-4 wt% Si, U235-69%	U-7Mo + ZrB ₂ dispersion in Al-4 wt% Si, U235-25%
	Bottom	A-5	A-6	A-7	A-8
		Aluminum Dummy	Aluminum Dummy	U-10Mo monolithic + B ₄ C-Al dispersion, U235-66%	U-10Mo monolithic + Al-1.5B alloy U235-66%
13-B	Top	B-1	B-2	B-3	B-4
		U-10Mo monolithic + ZrB ₂ -Al dispersion, U235-19.7%	U-10Mo monolithic + ZrB ₂ -Al dispersion, U235-66%	U-10Mo monolithic + B ₄ C-Al dispersion, U235-66%	U-10Mo monolithic + B ₄ C-Al dispersion, U235-19.7%
	Bottom	B-5	B-6	B-7	B-8
		Al-4.5B dispersion	Al-1.5B dispersion	ZrB ₂ -Al dispersion (Enriched B)	B ₄ C-Al dispersion
13-C	Top	C-1	C-2	C-3	C-4
		U-10Mo monolithic + ZrB ₂ -Al dispersion, U235-19.7%	U-10Mo monolithic + ZrB ₂ -Al dispersion, U235-66%	U-10Mo monolithic + B ₄ C-Al dispersion, U235-66%	U-10Mo monolithic + B ₄ C-Al dispersion, U235-19.7%
	Bottom	C-5	C-6	C-7	C-8
		Aluminum Dummy	Aluminum Dummy	U-10Mo monolithic + B ₄ C-Al dispersion, U235-66%	U-10Mo monolithic + Al-4.5B alloy, U235-66%
13-D	Top	D-1	D-2	D-3	D-4
		U-7Mo + B ₄ C dispersion in Al-4 wt% Si, U235-25%	U-7Mo + B ₄ C dispersion in Al-4 wt% Si, U235-69%	U-7Mo + ZrB ₂ dispersion in Al-4 wt% Si, U235-69%	U-7Mo + ZrB ₂ dispersion in Al-4 wt% Si, U235-25%
	Bottom	D-5	D-6	D-7	D-8
		Al-4.5B dispersion	Al-1.5B dispersion	ZrB ₂ -Al dispersion	B ₄ C-Al dispersion

2. Experimental

Table 2 enumerates the six samples that were characterized, their form, the specific analyses that have been performed to date, and the B-containing phase in the material. The laminate samples were fabricated by blending 400 mesh ($< 37 \mu\text{m}$) powders of B_4C and ZrB_2 powders (supplied by Ceradyne, Inc.) and aluminum powders, followed by compacting of the powders, and then rolling of the material to a desired thickness inside of an aluminum can. The edges of the can were then trimmed, leaving a layer of boron-bearing material sandwiched between two thin layers of AA6061 cladding. The single layer samples were fabricated by commercially procuring boron-bearing ingots from Ceradyne, Inc. and then rolling them to the desired thickness. The Al-4.5B (nominal wt% composition) ingot was manufactured by adding a boron halide to molten aluminum, and the Al-1.5B ingot was manufactured by adding a mixture of boron-halide and titanium-halide compounds to molten aluminum [1]. The single layer and laminate materials were inserted into fuel plates that were fabricated using the hot isostatic pressing (HIP) method [3]. All four samples (Al-1.5B, Al-4.5B, B_4C , and ZrB_2) were characterized in the unassembled (free foil) condition, and two samples (Al-1.5B and ZrB_2) were also analyzed in the as-HIPed condition.

The SEM analyses were conducted using a JEOL 7000F FEG SEM with energy-dispersive and wavelength-dispersive spectrometers (EDS/WDS) and a Zeiss Ultra-55 field emission SEM with X-ray energy dispersive spectroscopy (XEDS). Backscattered electron (BSE) imaging and X-ray mapping was performed on transverse cross sections of the samples to identify the microstructures and partitioning of the sample constituents amongst different phases. Specimens for TEM were prepared with a focused ion beam (FIB) in-situ (INLO) technique using a FEI™ TEM 200 FIB. The TEM analyses were performed using a FEI/Tecnai F30 300keV TEM/STEM equipped with a Fischione high-angle annular dark field (HAADF) detector. Electron diffraction was performed in the TEM to accurately identify the constituent phases based on crystal structure.

Table 1. Samples Employed for Microstructural Characterization

Label	Sample Form	Nominal B Loading (wt%)	Percentage of B that is B-10	Analysis Performed	B-Containing Phase
Al-1.5B	Single Layer	1.5	95.90	OM, SEM	AlB_2
Al-4.5B	Single Layer	4.5	98.50	OM, SEM	AlB_2
ZrB_2	Laminate	9.6	75.17	OM, SEM, TEM	ZrB_2
B_4C	Laminate	1.9	97.58	OM, SEM	B_4C
Al-1.5B HIP	HIP plate	1.5	95.90	OM, SEM, TEM	AlB_2
ZrB_2 HIP	HIP plate	9.6	75.17	OM, SEM	ZrB_2

3. Results

3.1 Al-1.5B and Al-1.5B HIP Sample

Figure 1 shows a BSE image of the microstructure observed for a section of the Al-1.5B sample. A heterogeneous distribution of precipitates was observed in the sample, along with relatively large areas of porosity. X-ray mapping of the sample demonstrated that the dark-contrast precipitates are enriched in Al, and the bright-phase precipitates are enriched in Ti. The Al-1.5B HIP sample had a similar microstructure without relatively large regions of porosity.

TEM analysis was performed on the Al-1.5B HIP sample. The bright contrast phases in the microstructure were comprised of Al_3Ti (larger particles) and AlTi_3 and Al_3Fe (smaller particles). The dark precipitates were AlB_2 .

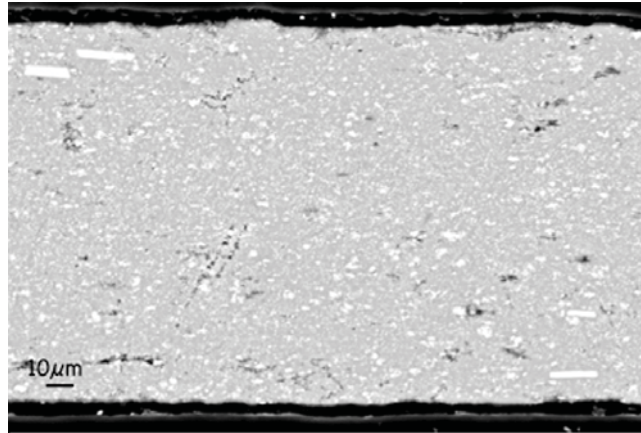


Fig. 1. BSE images of the microstructure observed for the Al-1.5B sample.

3.2 Al-4.5B Sample

Figure 2 shows a BSE image of the microstructure observed for a transverse cross section of the Al-4.5B sample. A heterogeneous distribution of precipitates were observed in the sample, along with relatively large areas of porosity. X-ray mapping of the microstructure demonstrated that the dark-contrast phases are enriched in Al and B.

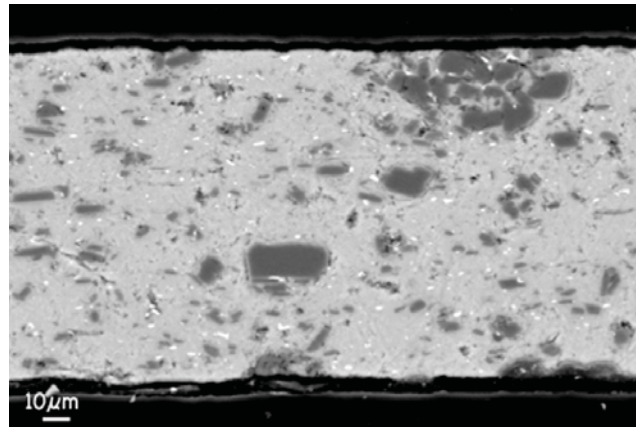


Fig. 2. BSE image of the microstructure observed for the Al-4.5B sample.

3.3 ZrB_2 and ZrB_2 HIP Sample

BSE images of the ZrB_2 sample microstructure are presented in Fig. 3. A generally uniform microstructure was observed with some areas of porosity. In the ZrB_2 HIP sample a similar microstructure was observed without any relatively large regions of porosity. TEM characterization of the ZrB_2 sample confirmed the presence of the ZrB_2 precipitate (bright contrast) and identified a minor $(\text{Al,Si})_{12}\text{Mg}_{17}$ precipitate (dark contrast).

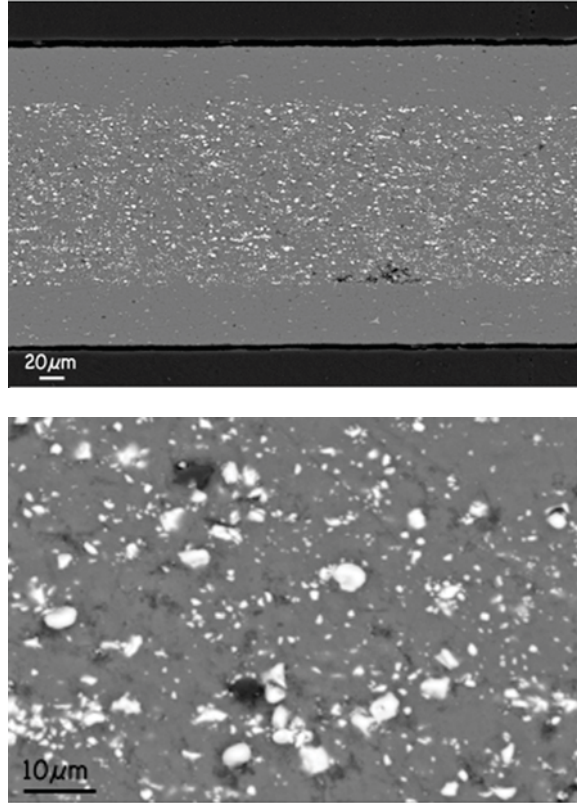


Fig. 3. BSE images of the microstructure observed for the ZrB_2 sample.

3.4 B_4C Sample

In Fig.4, the BSE image indicates that a fairly uniform microstructure was observed for the B_4C sample. The dark-contrast precipitates are the B_4C phase.

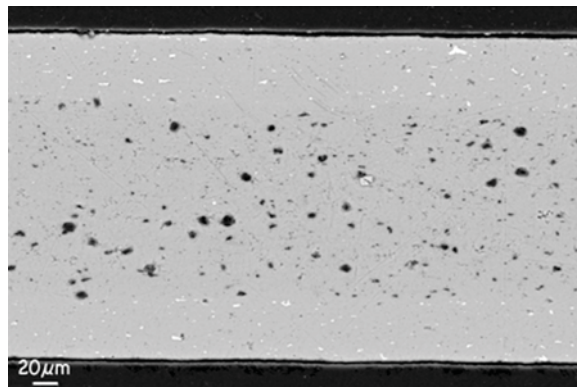


Fig. 4. BSE image of the microstructure observed for the B_4C sample.

4. Discussion

Microstructural characterization of Al-1.5B, Al-4.5B, ZrB₂, B₄C samples indicated that each sample has a very unique microstructure. The Al-1.5B sample has a significant fraction of Ti-containing precipitates and a minority AlB₂ phase that contains the boron. The Al-4.5B sample microstructure displays the AlB₂ phase as the majority phase, but there is a wide range in the size of the precipitates. The ZrB₂ sample has fairly uniform distribution of the ZrB₂ phase, but there is a fairly significant variation in the size of the precipitates. The B₄C sample also has a fairly uniform distribution of the B₄C phase and a fairly significant variation in the size of the precipitates.

When microstructural analysis is performed on the as-irradiated samples, it will be of particular interest to track the development of the porosity in the microstructure due to the generation of He from nuclear reactions with the boron contained in the different phases.

5. Conclusions

Based on the microstructural analyses performed on the BA samples that will be tested in the RERTR-13 experiment, there was a fairly significant difference in how the boron-containing phases were distributed in the various samples. The ZrB₂ and B₄C samples had the most uniform distribution of the boron-containing phases. The HIP process used to fabricate the final plate samples effectively closes porosity that was present in some of the foil samples in the as-rolled condition.

Acknowledgments

This work was supported by the U.S. Department of Energy, Office of Nuclear Materials Threat Reduction (NA-212), National Nuclear Security Administration, under DOE-NE Idaho Operations Office Contract DE-AC07-05ID14517.

References

- [1] I. Glagolenko et al., RERTR 2010, Lisbon, Portugal, Oct. 10-14, 2010.
- [2] A. Richt et al., Oak Ridge National Laboratory Report, ORNL-4714, (December, 1971).
- [3] Jan-Fong Jue et al., Nucl. Tech. 172 (2010) 204-210.